PHYSICAL REVIEW B **86**, 020409(R) (2012)

Anisotropic magnetoresistance in $Co_2(Fe,Mn)Si$ Heusler epitaxial films: A fingerprint of half-metallicity

F. J. Yang,[1,2] Y. Sakuraba,[1,*] S. Kokado,[3] Y. Kota,[4] A. Sakuma,[4] and K. Takanashi[1]

[1]*Institute for Materials Research, Tohoku University, Sendai 980-8577, Japan*

[2]*Faculty of Physics and Electronic Technology, Hubei University, Wuhan 430062, People's Republic of China*

[3]*Faculty of Engineering, Shizuoka University, Hamamatsu 432-8561, Japan*

[4]*Department of Applied Physics, Graduate School of Engineering, Tohoku University, Sendai 980-8579, Japan*

(Received 1 May 2012; revised manuscript received 26 June 2012; published 26 July 2012)

The anisotropic magnetoresistance (AMR) effect was systematically investigated in epitaxially grown $Co_2Fe_xMn_{1-x}Si$ films against Fe composition x and the annealing temperature. A change of sign in the AMR ratio from negative to positive was clearly detected when x increased from 0.6 to 0.8. This sign reversal can reasonably be explained by the change in the dominant s-d scattering process from $s\uparrow \rightarrow d\uparrow$ to $s\uparrow \rightarrow d\downarrow$ caused by the creation of large d-states at the Fermi level, suggesting the disappearance of half-metallicity at $x = 0.8$. The variations in the remanent density of states in the half-metallic gap against annealing temperature are also discussed from the viewpoint of the AMR ratio on the basis of the s-d scattering model.

DOI: 10.1103/PhysRevB.86.020409 PACS number(s): 75.76.+j, 85.75.−d

The anisotropic magnetoresistance (AMR) effect is one of the most conventional magnetoresistance effects in ferromagnets, in which the electric resistivity changes with a relative angle between the current and the magnetization directions. The AMR ratio is generally defined by

$$\frac{\Delta\rho}{\rho} = \frac{\rho_{\parallel} - \rho_{\perp}}{\rho_{\perp}},$$

where $\rho_{\parallel}(\rho_{\perp})$ represents the resistivity when the electric current flows parallel (perpendicular) to the magnetization. The AMR effect basically originates from s-d scattering from the conduction state (s-state) to localized d-states hybridized by spin–orbit interactions. Theories on what initiated the AMR effect were proposed by Campbell *et al.*[1] and Malozemoff,[2] in which resistivity due to s-d scattering from the s-state to the up-spin d-states ($d\uparrow$), down-spin d-states ($d\downarrow$), or both was taken into consideration. However, the difference in the s-d resistivity $\rho_{s\rightarrow d\uparrow}$ or $\rho_{s\rightarrow d\downarrow}$ between the up-spin s-state ($s\uparrow$) and the down-spin s-state ($s\downarrow$) was neglected in their formalizations,[3] even though such differences are essential to explain the AMR effect in highly spin-polarized ferromagnetic materials such as half-metallic materials. Kokado *et al.*[4] recently systematically investigated the relationship between the sign of the AMR ratio and the dominant s-d scattering process using an extended theory that specified the spin state of the s-state in s-d resistivity. As a result, they found that when the dominant s-d scattering process is $s\uparrow \rightarrow d\downarrow$ or $s\downarrow \rightarrow d\uparrow$, the sign of the AMR ratio tends to be positive ($\rho_{\parallel} > \rho_{\perp}$), as confirmed from body-centered cubic Fe, face-centered cubic Co, and Ni.[5] In contrast, when the dominant scattering is $s\uparrow \rightarrow d\uparrow$ or $s\downarrow \rightarrow d\downarrow$, the sign tends to be negative ($\rho_{\parallel} < \rho_{\perp}$), which is in good agreement with the AMR effect in Fe_4N.[6,7]

It is interesting to study the AMR effect in half-metallic materials on the basis of the theoretical prediction for the AMR effect by Kokado *et al.*[4] Because the density of states (DOS) in either up- or down-spin electrons at the Fermi level (E_F) is absent in half-metal, the sign of the AMR ratio should always be negative due to dominant $s\uparrow \rightarrow d\uparrow$ or $s\downarrow \rightarrow d\downarrow$ scattering. Half-metallic materials have recently attracted a great deal of interest in the spintronics field as an ideal spin-polarized current source for various kinds of spintronics devices, such as magnetic tunnel junctions (MTJs)[8–11] and giant-magnetoresistive devices;[12–15] thus, if the sign of the AMR ratio can be an indicator of half-metal or non-half-metal, it should be a useful technique to distinguish between half-metal and non-half-metal without any complicated microfabrication processes to make spintronic nanodevices. Negative AMR ratios have been reported in the epitaxial thin films of candidate half-metallic oxides such as $La_{0.7}Sr_{0.3}MnO_3$, $La_{0.7}Ca_{0.3}MnO_3$, and Fe_3O_4.[16,17] However, there have been no systematic investigations into the AMR effect in the films of half-metallic Heusler compounds such as Co_2MnSi (CMS), even though they are promising because of their high Curie temperature that is well beyond room temperature. The dependence of the Gilbert damping constant and tunneling magnetoresistance (TMR) on Fe composition has recently been systematically investigated in $Co_2Fe_xMn_{1-x}Si$ (CFMS) epitaxial films and those based on MTJs.[18,19] Consequently, a clear transition from a half-metallic to a non-half-metallic state has been confirmed around $x = 0.6$–0.8. Therefore, it is interesting to study the AMR effect in CFMS thin films with different Fe:Mn composition ratios systematically to clarify the relationship between half-metallicity and AMR ratio sign. The dependence of the AMR effect on the annealing temperature was also investigated in this Rapid Communication in CMS films to quantitatively analyze the AMR ratio.

We directly deposited 50-nm-thick CFMS films on (001)-oriented MgO substrates using an ultra-high-vacuum compatible sputtering system ($P_{base} \approx 3 \times 10^{-8}$ Pa). The compositions of the sputtering targets were adjusted to $Co_{43.7}Mn_{28.0}Si_{28.3}$ and $Co_{43.7}Fe_{28.0}Si_{28.3}$ to obtain a stoichiometric composition (i.e., Co:Mn (Fe):Si $\approx$ 2:1:1) in deposited films. The Fe compositions x in CFMS were set to 0.0, 0.2, 0.4, 0.6, 0.8, and 1.0 by cosputtering the CMS and Co_2FeSi (CFS) targets with a fixing sputtering rate of 0.03 nm/s. All CFMS films were annealed at 600 °C for 20 min to study x dependence. CMS films were annealed at various temperatures from 350 °C to 600 °C for 20 min to examine

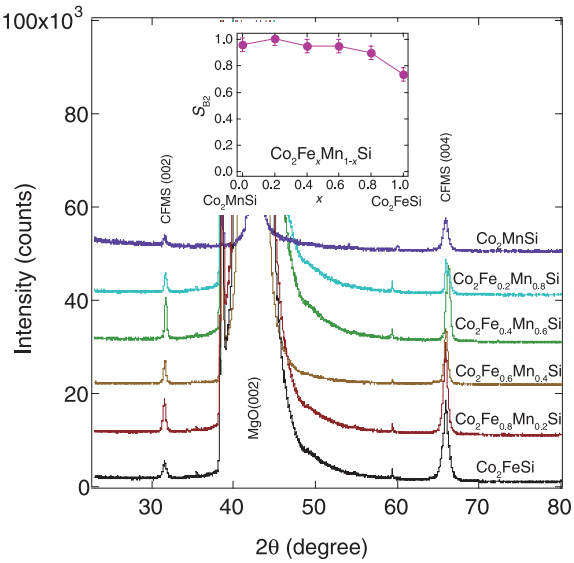

FIG. 1. (Color online) Dependence of XRD patterns on Fe composition x for CFMS films annealed at 600 °C. The inset indicates the dependence of the peak intensity ratio of (002) to (004) on x, suggesting degrees of B2 ordering.

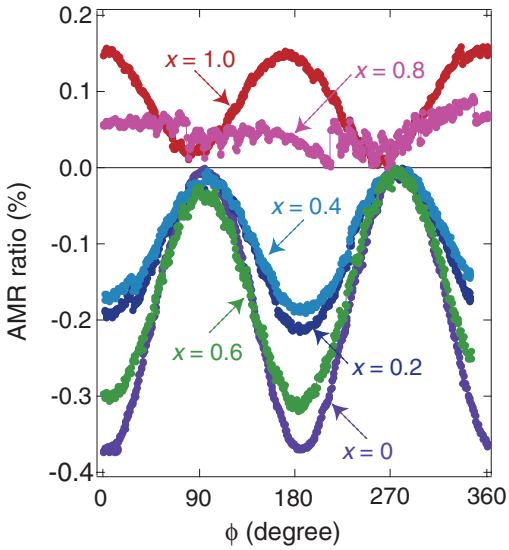

FIG. 2. (Color online) Dependence of the AMR ratio on the in-plane relative angle ϕ in $Co_2Fe_{1-x}Mn_xSi$ epitaxial films measured at 10 K.

annealing temperature dependence. The structural properties of the films were investigated with an x-ray diffractometer (XRD). The magnetization measurements of the films were carried out using a vibrating sample magnetometer. The AMR effect in all films was measured using a direct current (dc) four-terminal method by applying a dc current of 200 μA in the ⟨110⟩ in-plane direction of the CFMS film and rotating the direction of the external magnetic field on the film plane. A magnetic field of 3 kOe, which is high enough to saturate the magnetization of CFMS, was applied in all measurements. The relative angle between the directions of the magnetic field (i.e., magnetization) and the dc current is defined as ϕ.

The XRD patterns for the CFMS films with different x are shown in Fig. 1. For all x, only (002) and (004) peaks from the CFMS layer were confirmed, indicating (001)-oriented growth. Epitaxial growth was also confirmed by measuring the fourfold symmetry of (022) peaks in the ϕ-scan measurements. The degree of long-range B2 ordering (S_{B2}), which can be roughly estimated from the intensity ratio of the (002) superlattice to (004) fundamental peaks, is shown in the inset of Fig. 1. A highly ordered B2 structure ($S_{B2} > 0.75$) can be confirmed in all CFMS films with different x, which is important because B2 ordering is known to be a necessary condition to obtain half-metallic electronic structures.[20]

Figure 2 plots the dependence of the AMR ratio on ϕ for all CFMS films measured at 10 K, where the AMR ratio was calculated with $[(R(\theta) - R_\perp)R_\perp] \times 100(\%)$. Clear twofold symmetric curves can be observed for all x. Interestingly, the sign of the AMR ratio suddenly changed from negative to positive between $x = 0.6$ and $x = 0.8$. The sign of the AMR ratio does not change with temperature from 10 to 300 K in all CFMS films. Because no remarkable changes were observed in the structural analysis and magnetization measurements between $x = 0.6$ and $x = 0.8$, it is reasonable to consider the change in sign of the AMR ratio as originated from variations in the intrinsic electronic structure of CFMS.

Figure 3 plots the calculated spin-resolved DOS for CFMS with different x. The tight-binding linear muffin-tin orbital method within the framework of local spin density functional theory was used in the band calculations.[21,22] The partial disorder between Fe and Mn was treated by coherent potential approximation using Green's function technique. We found that CMS has a perfect half-metallic electronic structure from this calculation with an energy gap in the down-spin channel. In contrast, CFS has large d-states at E_F. The inset shows the dependence of the summation of d-states in CFMS on x at E_F. The number of d-states gradually increases with increasing x in the down-spin channel, in contrast to almost

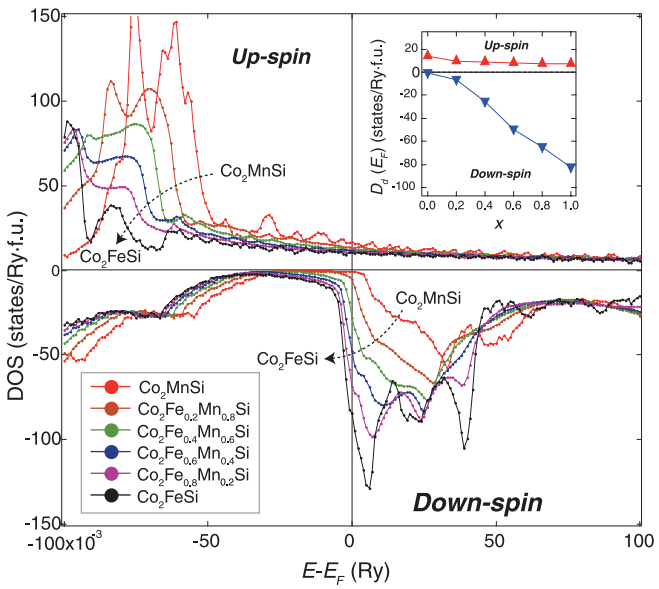

FIG. 3. (Color online) Spin-resolved DOS for CFMS ($x = 0.0$, 0.2, 0.4, 0.6, 0.8, and 1.0) in the B2 structure calculated from first principles. The inset indicates the dependence of the summation of partial d-states on Fe composition x in CFMS at E_F.

no change in the up-spin channel. A similar DOS was also predicted in CFMS by Galanakis *et al.*[23] Thus, from the *s*-*d* scattering model proposed by Kokado *et al.*[4] a change in sign of the AMR ratio from negative to positive is expected when a certain number of Fe atoms replaces Mn atoms, because dominant *s*-*d* scattering changes from $s\uparrow \rightarrow d\uparrow$ to $s\uparrow \rightarrow d\downarrow$. Therefore, it was concluded that the most likely reason for the observed sign reversal in the AMR ratio with $x = 0.6$–0.8 was the increase in *d*-states in the down-spin channel in the CFMS films. Previous experiments on the TMR effect and damping parameter using CFMS films also clearly demonstrated that CFMS has large *d*-states in the down-spin channel when x becomes 0.8;[8,18,19] i.e., the TMR ratio drastically decreased and the damping constant increased at $x = 0.8$, which agrees well with the preceding discussion based on the present results. Therefore, our observations of the AMR effect suggest that the sign of the AMR ratio can indicate high spin polarization originating from half-metallicity.[24] Previous theoretical studies on the DOS in CFS found the half-metallic electronic structure by using the local density approximation with Coulomb correlations.[25] However, the DOS, without considering the electron correlation shown in Fig. 3, agrees well with the AMR and TMR, at least in present and recent studies.[18,19]

The XRD patterns of CMS films with different annealing temperatures are plotted in Fig. 4. When the film was annealed at 350 °C, no CMS peaks except for the peaks from an MgO substrate were observed. After the annealing temperature was increased over 400 °C, (002) and (004) CMS peaks appeared. The epitaxial growth in all films was also confirmed by observing a fourfold symmetric (022) peak in the ϕ-scan measurements. The intensity ratio of the (002) superlattice to the (004) fundamental peak was almost constant above

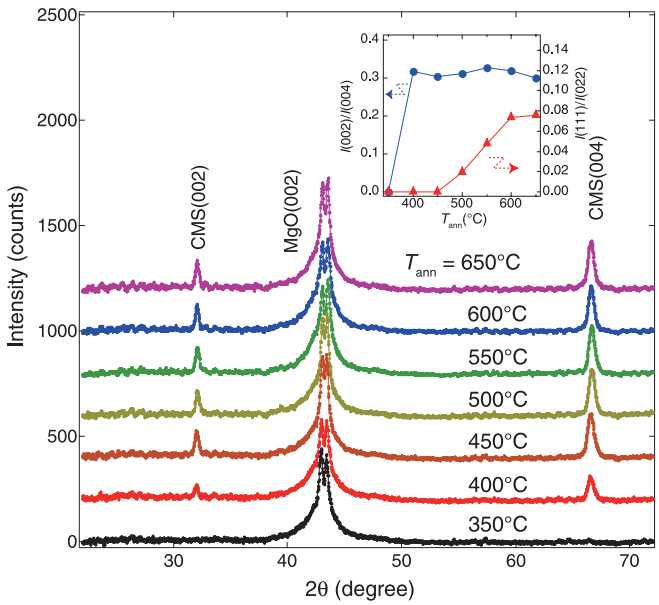

FIG. 4. (Color online) Dependence of XRD patterns on annealing temperature for CMS epitaxial films. The inset indicates the dependence of the peak intensity ratio of (002)–(004) and (111)–(022) on the annealing temperature, suggesting respective degrees of B2 and $L2_1$ ordering.

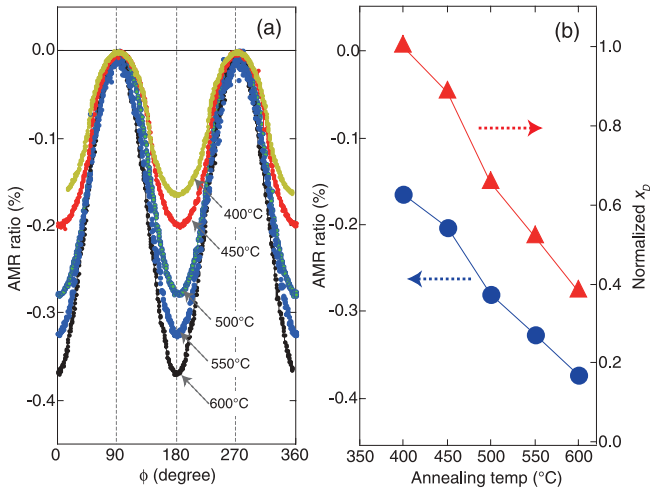

FIG. 5. (Color online) (a) Dependence of the AMR ratio on the in-plane relative angle ϕ in CMS epitaxial films with different annealing temperatures measured at 10 K. (b) Dependence of the AMR ratio on the annealing temperature in CMS epitaxial films and $x_D/(x_D)_{400}$.

400 °C, as can be seen in the inset of Fig. 4. The long-range order parameters of the B2 structure were estimated to be almost 0.9 for annealing temperatures above 400 °C, indicating nearly perfect B2 ordering. In contrast, the intensity ratio of the (111) superlattice peak to the (022) fundamental peak clearly increased with increasing annealing temperatures from 500 °C, indicating the promotion of $L2_1$ ordering with annealing beyond 500 °C. The long-range order parameter of the $L2_1$ structure estimated from the extended Webster model[26] was ∼0.68 at 600 °C.

Figure 5 plots the dependence of the AMR ratio on the relative angle ϕ measured for CMS films with different annealing temperatures. All highly B2-ordered CMS films indicate clear twofold symmetric curves with minima at $\phi = 0°$ and 180°, indicating negative AMR ratios. The observed AMR ratio of about -0.2% to -0.4% was almost the same as the value reported in other half-metallic materials.[16,27] Picozzi *et al.* predicted that the disordering between Mn and Si, i.e., B2-type disordering, does not affect half-metallic electronic structures.[20] Moreover, in a previous study on MTJs with a CMS electrode and an Al-O barrier,[28] high spin polarization over 0.9 was clearly confirmed in a highly B2-ordered CMS electrode with no $L2_1$ ordering. Therefore, negative AMR ratios from 400 °C to 600 °C are consistent with the prediction based on Kokado's model.[4] When we focus on the quantitative change in the AMR ratio against annealing temperature, we can clearly see that the magnitude of the AMR ratio gradually increased with increasing annealing temperature, as shown in Fig. 5(b). The most probable explanation for this increase is the change in DOS at E_F due to the enhancement of $L2_1$ chemical ordering, because the degree of $L2_1$ ordering seems to be the only parameter that changed remarkably with annealing. To find the change in DOS, we investigated the dependence of x_D ($= D_\downarrow/D_\uparrow$) on annealing temperature using Kokado's model,[4] where $D_\uparrow$ and $D_\downarrow$ were the majority-spin DOS and minority-spin DOS, respectively, at E_F. This x_D can be evaluated by substituting the measured AMR ratio

into an expression of the AMR ratio.[29] Figure 5(b) plots the dependence of $x_D/(x_D)_{400}$ on annealing temperature, where $(x_D)_{400}$ represents x_D at an annealing temperature of 400 °C. The calculated $x_D/(x_D)_{400}$ decreases by almost half with increasing annealing temperatures from 400 °C to 600 °C. Thus, this indicates that although a nearly half-metallic electronic structure was formed in the CMS film annealed at 400 °C, a small amount of minority-spin DOS remained in the half-metallic gap at 400 °C and gradually decreased by almost half with increasing annealing temperatures up to 600 °C, which is most likely due to the enhancement of $L2_1$ ordering.

In conclusion, we clearly observed a change in the sign of the AMR ratio from negative to positive in CFMS epitaxial films in this study when x increased from 0.6 to 0.8. This sign reversal can be well explained by the dominant s-d scattering process changing from $s\uparrow \rightarrow d\uparrow$ to $s\uparrow \rightarrow d\downarrow$, suggesting the disappearance of half-metallicity caused by the creation of large $d\downarrow$ states at E_F when $x = 0.8$. The magnitude of the AMR ratio gradually increased with increasing annealing temperature for CMS. Our analysis, based on the theoretical model, implies that a certain amount of remanent DOS in the half-metallic gap gradually decreased by almost half when the annealing temperature was increased from 400 °C to 600 °C. The AMR effect can be an indicator of half-metallicity or non-half-metallicity, which can easily be examined without having to make any microfabricated device structures.

Authors are grateful to T. Shima for the measurement in PPMS and M. Tsunoda for the useful discussions. This work was supported by MEXT/Grant-in-Aid for JSPS Fellows (21-09295), the Japan Science and Technology (JST) agency through its Strategic International Cooperative Program under the title "Advanced spintronic materials and transport phenomena (ASPIMATT)" and the Asahi Glass Foundation.

*y.sakuraba@imr.tohoku.ac.jp

[1] I. A. Campbell, A. Fert, and O. Jaoul, J. Phys. C Metal Phys. Suppl. **1**, S95 (1970).

[2] A. P. Malozemoff, Phys. Rev. B **32**, 6080 (1985).

[3] The spin dependence of the effective mass and the number density of electrons in the conduction band were neglected in an expression of $\rho_{s\rightarrow d\uparrow}$ or $\rho_{s\rightarrow d\downarrow}$. In contrast, Kokado's model (Ref. 4) takes into account their spin dependence, where the conduction band consists of the s, p, and conductive d-states.

[4] S. Kokado, M. Tsunoda, K. Harigaya, and A. Sakuma, J. Phys. Soc. Jpn. **81**, 024705 (2012).

[5] T. R. McGuire, J. A. Aboaf, and E. Klokholm, IEEE Trans. Magn. **20**, 972 (1984).

[6] M. Tsunoda, H. Takahashi, S. Kokado, Y. Komasaki, A. Sakuma, and M. Takahashi, Appl. Phys. Express **3**, 113003 (2010).

[7] M. Tsunoda, Y. Komasaki, S. Kokado, S. Isogami, C.-C. Chen, and M. Takahashi, Appl. Phys. Express **2**, 083001 (2009).

[8] Y. Sakuraba, M. Hattori, M. Oogane, H. Kubota, Y. Ando, H. Kato, A. Sakuma, and T. Miyazaki, Appl. Phys. Lett. **88**, 192508 (2006).

[9] S. Tsunegi, Y. Sakuraba, M. Oogane, K. Takanashi, and Y. Ando, Appl. Phys. Lett. **93**, 112506 (2008).

[10] T. Ishikawa, T. Marukame, H. Kijima, K.-I. Matsuda, T. Uemura, M. Arita, and M. Yamamoto, Appl. Phys. Lett. **89**, 192505 (2006).

[11] T. Taira, T. Ishikawa, N. Itabashi, K.-I. Matsuda, T. Uemura, and M. Yamamoto, J. Phys. D: Appl. Phys. **42**, 084015 (2009).

[12] T. M. Nakatani, T. Furubayashi, S. Kasai, H. Sukegawa, Y. K. Takahashi, S. Mitani, K. Kodama, and K. Hono, Appl. Phys. Lett. **96**, 212501 (2010).

[13] T. Iwase, Y. Sakuraba, S. Bosu, K. Saito, S. Mitani, and K. Takanashi, Appl. Phys. Express **2**, 063003 (2009).

[14] Y. Sakuraba, K. Izumi, T. Iwase, S. Bosu, K. Saito, K. Takanashi, Y. Miura, K. Futatsukawa, K. Abe, and M. Shirai, Phys. Rev. B **82**, 094444 (2010).

[15] Y. K. Takahashi, A. Srinvasan, B. Varaprasad, A. Rajanikanth, N. Hase, T. M. Nakatani, S. Kasai, T. Furubayashi, and K. Hono, Appl. Phys. Lett. **98**, 152501 (2011).

[16] M. Ziese, Phys. Rev. B **62**, 1044 (2000).

[17] E. Favre-Nicolin and L. Ranno, J. Magn. Magn. Mater. **272–276**, 1814 (2004).

[18] T. Kubota, S. Tsunegi, M. Oogane, S. Mizukami, T. Miyazaki, H. Naganuma, and Y. Ando, Appl. Phys. Lett. **94**, 122504 (2009).

[19] M. Oogane, T. Kubota, Y. Kota, S. Mizukami, H. Naganuma, A. Sakuma, and Y. Ando, Appl. Phys. Lett. **96**, 252501 (2010).

[20] S. Picozzi, A. Continenza, and A. J. Freeman, Phys. Rev. B **69**, 094423 (2004).

[21] O. K. Andersen, Phys. Rev. B **12**, 3060 (1975).

[22] J. Kudrnovský and V. Drchal, Phys. Rev. B **41**, 7515 (1990).

[23] I. Galanakis, K. K. Özdoğan, B. Aktaş, and E. Şaşıoğlu, Appl. Phys. Lett. **89**, 042502 (2006).

[24] We also carried out the supplemental investigation of the AMR ratio in CMS and CFS compounds with the B2 structure by first-principles calculation of the electric conductivities employing the Kubo-Greenwood formula to verify the results of the experiment and the theoretical analysis in this study. The calculated results show that the AMR ratio exhibits a negative sign in half-metallic CMS and a positive one in non-half-metallic CFS. The absolute values of these AMR ratios are below 1%, which is adequately consistent with the experimental results; however, this means that these calculations require high accuracy. More precise calculations are being carried out.

[25] S. Wurmehl, G. H. Fecher, H. C. Kandpal, V. Ksenofontov, C. Felser, H. J. Lin, and J. Morais, Phys. Rev. B **72**, 184434 (2005).

[26] Y. Takamura, R. Nakane, and S. Sugahara, J. Appl. Phys. **105**, 07B109 (2009).

[27] M. Ziese and S. P. Sena, J. Phys. Condens. Matter **10**, 2727 (1998).

[28] Y. Sakuraba, M. Hattori, M. Oogane, H. Kubota, Y. Ando, A. Sakuma, N. D. Telling, P. Keatley, G. van der Laan, E. Arenholz, R. J. Hicken, and T. Miyazaki, J. Magn. Soc. Jpn. **31**, 338 (2007).

[29] The expression of the AMR ratio is given by Eq. (62) of Ref. 4. For parameters in Eq. (62), we set $\gamma = 0.01$ and $u = 1$ as typical values. In addition, $m^*_\downarrow/m^*_\uparrow$ is chosen to be 0.01–0.1 on the basis of the effective mass of the carrier of a typical semiconductor divided by the electron mass (Ref. 30). In this case, the $m^*_\downarrow/m^*_\uparrow$ dependence of $x_D/(x_D)_{400}$ is negligible small.

[30] C. Kittel, *Introduction to Solid State Physics* (John Wiley & Sons, New York, 1986) 6th ed., p. 193, and Table 2, p. 198.